Nonlocal electronic correlations in the cohesive properties of high-pressure hydrogen solids

Ting Ting Cui,[1] Jian Chen Li,[1] Wang Gao,[1,*] Jan Hermann,[2] Alexandre Tkatchenko,[2,*] Qing Jiang[1,*]
[1]*Key Laboratory of Automobile Materials (Jilin University), Ministry of Education, Department of Materials Science and Engineering, Jilin University, Changchun 130022, China and*
[2]*Physics and Materials Science Research Unit, University of Luxembourg, L-1511 Luxembourg**
(Dated: July 8, 2019)

High-pressure hydrogen exhibits remarkable phenomena including the insulator-to-metal (IM) transition, however, a complete resolution of its phase diagram is still an elusive goal despite many efforts and much controversy. Theoretical modeling is typically based on density-functional theory (DFT) with a mean-field description of electronic correlations, which is known to be rather limited in describing IM transitions. Herein, we show that nonlocal electron correlations play a central role in the relative stability of solid hydrogen phases, and that DFT corrected for these correlations by the many-body dispersion (MBD) model reaches the accuracy of quantum Monte–Carlo (QMC) simulations and predicts the same $C2/c$-24→$Cmca$-12→Cs(IV) IM transition. In contrast with the conventional assumption that many-body electronic correlations become localized in metallic systems because of exponential screening with interelectronic distance, we find that the anisotropy of electronic response of hydrogen solids under pressure leads to longer-ranged many-body effects in metallic phases relative to insulating ones. This reshapes our understanding of phase diagram of hydrogen solids as well as anisotropic many-body correlations.

Despite its apparent simplicity, hydrogen forms diverse high-pressure solid and liquid phases [1, 2], which exhibit remarkable physical phenomena such as the insulator-to-metal (IM) transition or dissipationless quantum states, including metallic and superconducting superfluids [3–9]. Due to its consequences for astrophysics as well as out of sheer fundamental interest, the characterization of the phase diagram of dense hydrogen has attracted much effort. Yet, while many of the phases and the transitions between them have been determined beyond any doubt, a large portion of the phase diagram remains unresolved, and experiments pushing the pressure boundaries further often turn out to be controversial.

The characterization of the crystal and electronic structure of the solid phases of hydrogen is essential for our understanding of its high-pressure behavior. Experimental difficulties at the required level of pressure stem from the instability of even the hardest materials such as diamond to mechanical and chemical strain, as well as from the limitations of common characterization techniques [2, 10–12]. There is a wide consensus on the general shape of the low-temperature part of the hydrogen phase diagram below 250 GPa, which comprises phases I to IV, but only the crystal structure of phase I has been experimentally fully resolved, with several available restrictions on the possible structure of phases II and III. Molecular solid hydrogen is expected to undergo the IM transition at extreme pressure, and indirect experimental evidence suggests that this does not occur before reaching at least 450 GPa at zero temperature [6]. Recent experiments reported the transition of phase III to a nonmetallic molecular phase at 350 GPa and, furthermore, the transition to an atomic metal at 495 GPa [13, 14]. However, these claims have been disputed and no general consensus has yet been reached on the matter [15].

On the modeling side, the major obstacles are sufficient exploration of the configuration space, the accuracy of electronic-structure methods, and the effect of zero-point motion (ZPM). Density-functional theory (DFT) and quantum Monte–Carlo (QMC) calculations proved to be the two most successful methods to account for the electronic energy in solid hydrogen [16–20], with the former often serving for the candidate structure search because of its high computational efficiency, and the latter for more reliable estimates of the stability of different phases because of its ability to capture many-body electronic correlation. The common thread in comparisons of DFT and QMC calculations is their different prediction of the progression with pressure from phase III to the conjectured metallic atomic Cs(IV) phase (not to be confused with phase IV). Whereas QMC predicts the transition via a single $Cmca$-12 phase, DFT calculations, regardless whether corrected for pairwise van der Waals (vdW) interactions and ZPM, suggest unambiguously that $Cmca$-12 is first followed by a semimetallic molecular $Cmca$-4 phase before the Cs(IV) phase is reached [17–19]. The DFT results are in contradiction not only with QMC, but also with experiment, which suggests that there is at most one additional transition between phase III and the IM transition, and that all potential molecular phases preceding the IM transition are nonmetallic. In this light, it is crucial to understand how many-body electronic correlations and their response to pressure depend on the metallic or insulating nature of hydrogen solid phases.

In this contribution, we uncover the essential role of nonlocal electron correlations in the relative stability of high-pressure hydrogen phases, and demonstrate that DFT corrected for these correlations gives predictions in agreement with QMC simulations. To this end, we

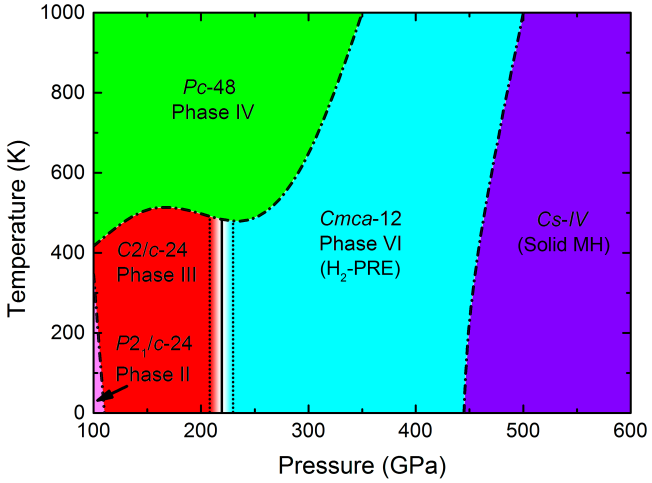

FIG. 1: Pressure–temperature phase diagram of solid hydrogen as calculated with the PBE+MBD method. The dotted lines indicate the uncertainty in the phase boundaries.

use the many-body dispersion (MBD) method [21, 22], which is able to capture these nonlocal correlations at much lower computational cost than QMC, while providing a simple enough model that is amenable to further analysis and interpretation. In contrary to the conventional assumption that the exponential screening of metallic systems with interelectronic distance generates localized many-body electronic correlations, we find that the anisotropy of electronic response of hydrogen solids under pressure leads to longer-ranged many-body effects in metallic phases relative to insulating ones. This leads to different nonlocal electron correlations between metallic phases and insulating phases of hydrogen solids at pressure as high as 500 GPa, reordering their relative stability, and thus qualitatively changing the phase diagram. We attribute the difficulty in the estimation of the electronic energy of high-pressure hydrogen phases to the nontrivial interplay between the mean-field, many-body, and collective character of the nonlocal electronic fluctuations. In insulators and semiconductors, any nonlocal fluctuations stem solely from many-body vdW interactions, while in normal metals the electronic interactions can be separated into a local mean-field description and collective nonlocal fluctuations—plasmons [23]. In the high-pressure hydrogen phases, however, the boundary between vdW and plasmonic fluctuations becomes less clear, which makes both semilocal DFT and pairwise vdW methods insufficient for their description. Our results suggest that the MBD model is able to effectively capture this unusual range of nonlocal fluctuations at least on the energetic level, but more work will be required for full understanding of the detailed electronic structure.

We start by calculating the pressure–temperature phase-diagram of solid hydrogen with the exchange–correlation functional of Perdew, Burke, and Ernzerhof [24] augmented with MBD method (PBE+MBD) within the harmonic approximation (Fig. 1). The general order of individual phases with respect to pressure and temperature agrees well with the experimentally obtained phase diagrams [14], which has been so far unattainable for DFT-based approaches. In particular, PBE+MBD predicts a single phase between the molecular phase III and the metallic atomic Cs(IV) phase. In what follows, we compare the predictions of DFT+MBD to other DFT+vdW approaches, and analyze the theoretical reasons for the observed differences in detail.

We evaluate the relative stabilities of hydrogen solid phases with different DFT+vdW methods, focusing on molecular $C2/c$-24 (phase III), $Cmca$-12, and $Cmca$-4, and atomic metallic Cs(IV) [Fig. 2(a)], with two other structures corresponding to phases II and IV shown in Fig. S1 in Supplemental Materials (SM). The PBE+MBD method predicts the transition $C2/c$-24→$Cmca$-12→Cs(IV), indicating that the metallic $Cmca$-4 is never energetically stable with respect to the insulating $Cmca$-12, in agreement with QMC calculations and circumstantial experimental evidence [13, 14] [Fig. 2(b)]. In contrast, the bare PBE functional as well as two pairwise vdW methods, PBE+TS [25] and PBE+D2 [26] (see Methods in SM), consistently predict that the metallic $Cmca$-4 is energetically preferred over $Cmca$-12 in a certain range of pressures preceding the IM transition. Using a three-body correction to the pairwise vdW interactions, PBE+D3 [27] eliminates $Cmca$-4, but at the price of eliminating also $Cmca$-12 and shifting the IM transition to unrealistically low pressure. Since PBE is exact in the high-density limit, it is in general assumed to be suitable for high-pressure systems, and indeed, pairwise vdW interactions seem relatively negligible. But our results demonstrate that the long-range many-body correlations are in fact essential for the relative stability of hydrogen solids, and accounting for them effectively brings the predictive power of semilocal DFT up to par with QMC.

We have further investigated the effect of the self-interaction error (SIE) and of the ZPM on the phase-diagram predictions. The former can be largely mitigated by using the functional of Heyd, Scuseria, and Ernzerhof (HSE) [28] instead of PBE, which increases the pressure estimates by 50 and 100 GPa for the $C2/c$-24→$Cmca$-12 and $Cmca$-12→Cs(IV) transitions, respectively. We treat the ZPM in the harmonic approximation (see Fig. S2 in SM), and find that it narrows the window of stability of $Cmca$-12 on both ends. Most importantly, neither the SIE nor ZPM affect the phase-diagram predictions qualitatively, in the sense that the semimetallic $Cmca$-4 does not become stable at any point. Quantitatively, the transition pressures become only more accurate by accounting for the SIE and ZPM with respect to the experimentally conjectured values.

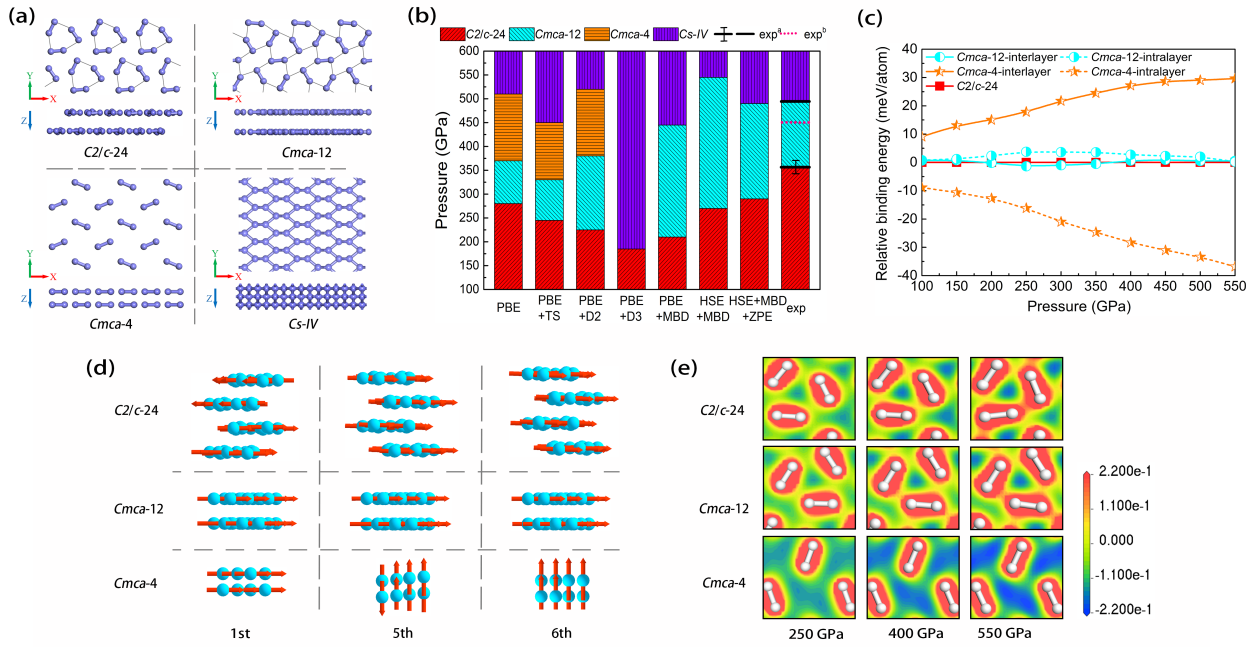

FIG. 2: Phase-transition pressure of hydrogen solids and corresponding energetics and geometric/electronic structures. (a) Crystal structures of the four hydrogen phases viewed perpendicular to (top) and along (bottom) the layers. (b) Transition pressure between the four hydrogen phases as predicted by different theoretical methods along with experimental results. (c) Inter- and intralayer MBD binding energy in *Cmca*-12 and *Cmca*-4 relative to the corresponding part in $C2/c$-24. (d) Schematic illustration of several representative (1st, 5th, and 6th) low-energy collective MBD fluctuations for $C2/c$-24, *Cmca*-12, and *Cmca*-4 at 400 GPa. (e) Electron density difference between a hydrogen solid and a superposition of noninteracting hydrogen molecules. Red/blue denotes accumulation/depletion of electron density due to intermolecular interactions.

The contribution of the nonlocal correlations can be decomposed according to the present binding patterns. All three studied molecular phases have a layered crystal structure, and the largest contribution to the absolute binding energies comes from *inter*layer interactions. But analysis of the binding energy reveals that it is the difference in the *intra*layer MBD energy between different phases that destabilizes the *Cmca*-4 phase with respect to the two insulating molecular phases [Fig. 2(c)]. These effects can be further understood based on the analysis of the MBD Hamiltonian wave function, which is presented below.

MBD describes vdW energy in terms of collective charge-density fluctuation modes, which range from fluctuations extended over the whole system and resembling molecular dipoles or higher multipoles [29], to wave-like dipole fluctuations in low-dimensional nanomaterials [30]. This picture is in stark contrast to the standard London dispersion, in which all fluctuations are localized on individual atoms and correlated in a pairwise fashion. All three molecular hydrogen phases considered here have wave-like dipole fluctuations as the lowest-energy modes [Fig. 2(d)]. Interestingly, the fluctuations are preferentially in-plane in the insulating phases, but out-of-plane in the semimetallic phase. This observation is aligned with the difference in the inter- and intralayer binding energies between the three phases [Fig. 2(c)]. Accordingly, there is a difference in the electron density polarization due to the intermolecular interactions between the insulating and semimetallic phases [Fig. 2(e)]. In the insulating phases, the electron density accumulates between the molecules within each layer with increasing pressure. In the semimetallic phase, on the other hand, the density is channeled into the interlayer space with increasing pressure. This indicates that the layered nature of the two insulating phases is like that of graphite and differs significantly from that of the molecular semimetallic phase.

To better understand the effect of the collective fluctuations on the stability of the solid hydrogen phases, we compare the behavior of binding energies and C_6 coefficients between the pairwise TS model and MBD (see Methods in SM for details). The many-body effects can induce both polarization and depolarization depending on the dimensionality and topology of the system—it usually enhances the polarizability of low-dimensional nanomaterials but depolarizes bulk compounds. The difference in the TS energy between different phases depends only weakly on pressure [Fig. 3(a)]. In contrast, the difference in the MBD energy ranges from 2 to 20 meV/atom and depends strongly on pressure [Fig. 3(b)], significantly altering the relative stability of hydrogen solids. Partially responsible for this dif-

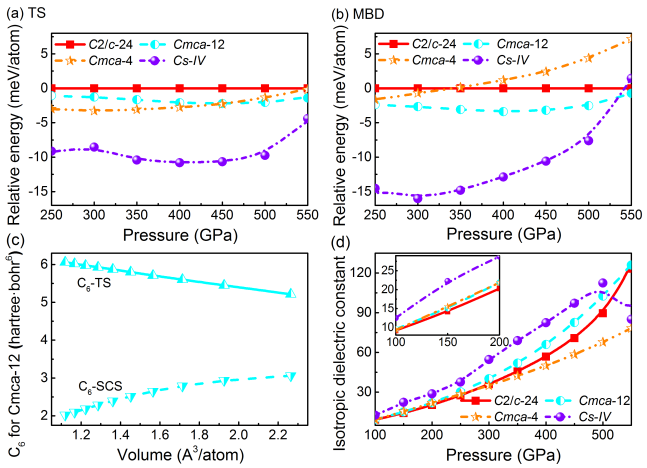

FIG. 3: Differences in vdW energy of hydrogen solids and in the corresponding C_6 coefficient and isotropic relative permittivity. (a,b) Contribution to enthalpy from the TS and MBD models relative to $C2/c$-24. (c) C_6 coefficients (a.u.) of a hydrogen atom in $Cmca$-12 as calculated by the pairwise TS model and the many-body self-consistent screening (SCS) equation [21, 22, 31]. (d) Static isotropic relative permittivity of hydrogen phases.

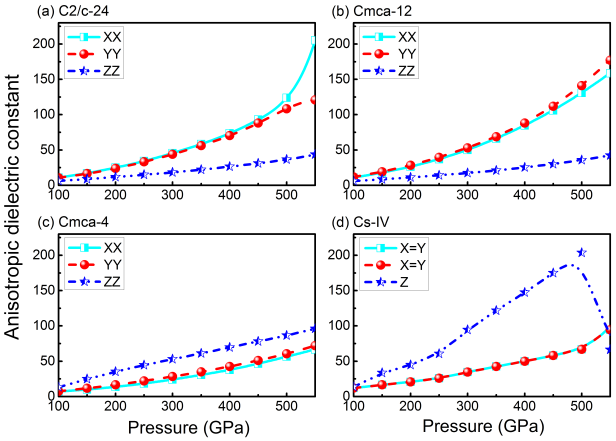

FIG. 4: Anisotropic relative permittivity of different hydrogen phases as a function of pressure. The results are calculated with the MBD model. (a)-(d) denote the different phases. The Cartesian axes are aligned with the lattice vectors.

ference is the dependence of the C_6 coefficients of the hydrogen atoms on atomic volume [Fig. 3(c)]. Whereas this is strictly linear by construction in the case of TS, the dependence is significantly stronger at high pressures (low volumes, see Fig. S3 in SM) in the case of MBD [21, 22, 31]. Finally, the difference in the MBD energy between the phases can be directly attributed to the metallicity of a given phase. With increasing pressure, the MBD energy difference between the insulating $Cmca$-12 and $C2/c$-24 is negligible (below 3 meV/atom), and that between the semimetallic $Cmca$-4 and Cs(IV) remains in a narrow range, especially at 300–500 GPa (∼15 meV/atom). In contrast, the difference between these two groups depends strongly on pressure. This difference in stability can be mapped directly to the difference in the nature of the vdW many-body fluctuations in the different phases.

Although the long-range dipole fluctuations cannot be directly associated with the electronic plasmons, they do capture the underlying long-range order in the electronic motion [29]. An effective tool to compare the nature of the fluctuations between different crystal structures is the density of states (DOS) of the coupled oscillators. In particular, the DOS of the coupled oscillations has substantially narrower dispersion in the metallic phases, signifying fluctuations that are dominated by longer-ranged interactions that are independent of local crystal geometry (see Fig. SX in SM). In contrast, the insulating phases have a wider and more structured DOS, which is governed by the relative positions of the neighboring molecules in the crystal. The longer-ranged many-body effects destabilize metallic $Cmca$-4 with respect to insulating $Cmca$-12 and $C2/c$-24, in stark contrast with the conventional wisdom that metallic systems possess localized many-body electronic correlations because of exponential screening with interelectronic distance. This is induced by the anisotropy of electronic response of hydrogen solids under pressure as shown below.

While the MBD fluctuation modes are useful for understanding the vdW binding, they exist only within the model and are not directly measurable. However, the anisotropy in the modes [Fig. 2(d)] should directly translate into anisotropy in observable quantities. To demonstrate this, we calculate the relative permittivity of solid phases of hydrogen as a function of pressure [Fig. 3(d) and 4, see Methods in SM for details]. Whereas the difference in the isotropic permittivity between phases is merely qualitative, the difference in anisotropy is quantitative. The strong in-plane fluctuation modes of the molecular insulating phases translate into large in-plane and small out-of-plane permittivity, especially at large pressure. In contrast, the difference in permittivity between different directions remains constant across all pressures for the molecular semimetallic phase, in line with both in-plane and out-of-plane fluctuation modes being present at low energies. In the metallic Cs(IV) phase, the relationship is reversed, and it is the out-of-plane direction that is dominantly polarizable.

Apart from the theoretical motivation, relative permittivity can be readily measured, and thus serve as an indicator for experimental characterization of the solid phases. The MBD results obtained here for $Cmca$-12 at 100–200 GPa agree well with the results from Bethe–Salpeter equation and GW approximation [32, 33] (see Table SI in SM). Our calculations suggest that the IM

transition is associated with a prominent change in the anisotropy of the relative permittivity, going from two strongly polarizable axes to a single strongly polarizable axis. The calculated static relative permittivity of the Cs(IV) phase is ∼100 at 450–500 GPa, leading to the reflectance of 0.90, which is consistent with the experimental values of 0.90±0.05 at 495±13 GPa [14]. Our results thus suggest that Cs(IV) is the structure of the atomic metallic hydrogen observed experimentally.

Our calculations demonstrate that the long-range many-body vdW interactions are essential for the correct description of phase behavior of solid hydrogen. Using a collective charge-density fluctuation model, we find evidence that metallic hydrogen phases surprisingly exhibit longer-ranged many-body effects with respect to insulating hydrogen ones, consequently determining the mechanical stability and response to pressure of solid hydrogen phases. The HSE+MBD approach coupled with quasi-harmonic ZPM gives stability predictions in agreement with the much more costly QMC calculations and available experimental results. Moreover, the anisotropy of the relative permittivity as predicted by MBD could serve as an experimentally available descriptor of different solid phases of hydrogen.

We gratefully acknowledge support from the Young Thousand Talents Program of China, the National Natural Science Foundation of China (No. 21673095, 51631004), JLU Science and Technology Innovative Research Team (No. 2017TD-09), the fund of "World-class Universities and World-class Disciplines", and the computing resources of High Performance Computing Center of Jilin University, China.

* Electronic address: wgao@jlu.edu.cn;alexandre.tkatchenko@uni.lu;jiangq@jlu.edu.cn

[1] H.-k. Mao and R. J. Hemley, Rev. Mod. Phys. **66**, 671 (1994).
[2] J. M. McMahon, M. A. Morales, C. Pierleoni, and D. M. Ceperley, Rev. Mod. Phys. **84**, 1607 (2012).
[3] N. W. Ashcroft, Phys. Rev. Lett. **21**, 1748 (1968).
[4] E. Babaev, A. Sudbø, and N. W. Ashcroft, Nature **431**, 666 (2004).
[5] S. Deemyad and I. F. Silvera, Phys. Rev. Lett. **100**, 155701 (2008).
[6] P. Loubeyre, F. Occelli, and R. LeToullec, Nature **416**, 613 (2002).
[7] S. A. Bonev, E. Schwegler, T. Ogitsu, and G. Galli, Nature **431**, 669 (2004).
[8] P. Cudazzo, G. Profeta, A. Sanna, A. Floris, A. Continenza, S. Massidda, and E. K. U. Gross, Phys. Rev. Lett. **100**, 257001 (2008).
[9] J. M. McMahon and D. M. Ceperley, Phys. Rev. B **84**, 144515 (2011).
[10] A. F. Goncharov, E. Gregoryanz, R. J. Hemley, and H.-k. Mao, Proc. Natl. Acad. Sci. USA **98**, 14234 (2001).
[11] M. I. Eremets and I. A. Troyan, Nat. Mater. **10**, 927 (2011).
[12] R. T. Howie, C. L. Guillaume, T. Scheler, A. F. Goncharov, and E. Gregoryanz, Phys. Rev. Lett. **108**, 125501 (2012).
[13] R. Dias, O. Noked, and I. F. Silvera, arXiv preprint arXiv:1603.02162 (2016).
[14] R. P. Dias and I. F. Silvera, Science **355**, 715 (2017).
[15] X.-D. Liu, P. Dalladay-Simpson, R. T. Howie, B. Li, and E. Gregoryanz, Science **357**, eaan2286 (2017).
[16] M. A. Morales, J. M. McMahon, C. Pierleoni, and D. M. Ceperley, Phys. Rev. Lett. **110**, 065702 (2013).
[17] N. D. Drummond, B. Monserrat, J. H. Lloyd-Williams, P. L. Ríos, C. J. Pickard, and R. J. Needs, Nat. Commun. **6**, 7794 (2015).
[18] J. McMinis, R. C. Clay III, D. Lee, and M. A. Morales, Phys. Rev. Lett. **114**, 105305 (2015).
[19] G. Mazzola and S. Sorella, Phys. Rev. Lett. **114**, 105701 (2015).
[20] S. Azadi, B. Monserrat, W. M. C. Foulkes, and R. J. Needs, Phys. Rev. Lett. **112**, 165501 (2014).
[21] A. Tkatchenko, R. A. DiStasio Jr, R. Car, and M. Scheffler, Phys. Rev. Lett. **108**, 236402 (2012).
[22] A. Ambrosetti, A. M. Reilly, R. A. DiStasio Jr, and A. Tkatchenko, J. Chem. Phys. **140**, 18A508 (2014).
[23] D. Pines and D. Bohm, Phys. Rev. **85**, 338 (1952), 00945.
[24] J. P. Perdew, K. Burke, and M. Ernzerhof, Phys. Rev. Lett. **77**, 3865 (1996).
[25] A. Tkatchenko and M. Scheffler, Phys. Rev. Lett. **102**, 073005 (2009).
[26] S. Grimme, Journal of Computational Chemistry **27**, 1787 (2006).
[27] S. Grimme, J. Antony, S. Ehrlich, and H. Krieg, The Journal of Chemical Physics **132**, 154104 (2010).
[28] J. Heyd, G. E. Scuseria, and M. Ernzerhof, J. Chem. Phys. **124**, 219906 (2006).
[29] J. Hermann, D. Alfe, and A. Tkatchenko, Nat. communications **8**, 14052 (2017).
[30] A. Ambrosetti, N. Ferri, R. A. DiStasio, and A. Tkatchenko, Science **351**, 1171 (2016).
[31] G.-X. Zhang, A. Tkatchenko, J. Paier, H. Appel, and M. Scheffler, Phys. Rev. Lett. **107**, 245501 (2011).
[32] M. Dvorak, X.-J. Chen, and Z. Wu, Phys. Rev. B **90**, 035103 (2014).
[33] S. Lebègue, C. M. Araujo, D. Y. Kim, M. Ramzan, H.-k. Mao, and R. Ahuja, Proc. Natl. Acad. Sci. USA **109**, 9766 (2012).